

# Reactions of Platina- $\beta$ -diketones with 2-Aminopyridines: Synthesis and Characterization of Aminocarbene Complexes of Platinum(II)

Tushar Gosavi, Christoph Wagner, Kurt Merzweiler, Harry Schmidt, and Dirk Steinborn\*

*Institut für Anorganische Chemie, Martin-Luther-Universität Halle-Wittenberg, Kurt-Mothes-Strasse 2, D-06120 Halle, Germany*

Received October 19, 2004

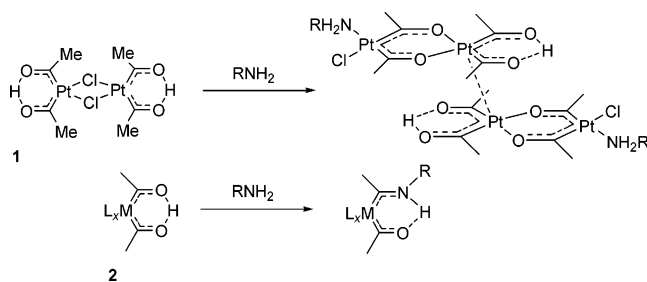
Reactions of the dinuclear platina- $\beta$ -diketone [Pt<sub>2</sub>{(COMe)<sub>2</sub>H}<sub>2</sub>( $\mu$ -Cl)<sub>2</sub>] (**1**) with 2-aminopyridine and 2-(*N*-methylamino)pyridine resulted in the formation of cyclic aminocarbene complexes of platinum(II) [Pt(COMe)Cl{2-(CMe=NR)C<sub>5</sub>H<sub>4</sub>N- $\kappa$ C,N}] (R = H, **3a**; Me, **3b**). Constitution of these complexes was confirmed by microanalysis and IR and NMR (<sup>1</sup>H, <sup>13</sup>C) spectroscopy. Single-crystal X-ray diffraction analyses of **3a** and **3b** showed them to be monomeric square-planar platinum complexes with the chloro ligand trans to the carbene ligand (configuration index *SP*-4-4). The five-membered platinacycles Pt–C–N–C–N are planar in good approximation. The bond lengths Pt–C<sub>carbene</sub> (1.943(6)–1.950(9) Å) and N–C<sub>carbene</sub> (1.31(1)–1.340(7) Å) indicate some double-bond character as further established by DFT calculations. A tentative mechanism for the formation of the aminocarbene complexes **3a/b** is discussed.

## 1. Introduction

The dinuclear platina- $\beta$ -diketone [Pt<sub>2</sub>{(COMe)<sub>2</sub>H}<sub>2</sub>( $\mu$ -Cl)<sub>2</sub>] (**1**), prepared by the reaction of hexachloroplatinic(IV) acid with the alkynylsilane Me<sub>3</sub>Si–C $\equiv$ C–SiMe<sub>3</sub> in *n*-butanol, can be regarded as a hydroxycarbene complex stabilized by a strong intramolecular hydrogen bond to an acyl ligand.<sup>1</sup> It is an electronically unsaturated complex (16 ve; ve = valence electrons) with a kinetically labile ligand sphere. This is why complex **1** exhibits an entirely different reactivity than Lukehart's mononuclear metalla- $\beta$ -diketones [L<sub>x</sub>M{(COR)<sub>2</sub>H}] (**2**) (L = CO, Cp; M = Mo, Re, Fe, ...; R = alkyl, aryl), which are electronically saturated (18 ve) and kinetically stable complexes.<sup>2</sup> The pronounced different reactivity is demonstrated in Scheme 1 in reactions with amines, affording in the case of complex **1** platina- $\beta$ -diketonates of platina- $\beta$ -diketones.<sup>3</sup> On the other hand Lukehart's metalla- $\beta$ -diketones **2** were found to react with amines analogously to Fischer carbene complexes with formation of metalla- $\beta$ -ketoimines (Scheme 1).<sup>2</sup>

Typically, with chelating ligands complex **1** was found to react with bridge cleavage (**1**  $\rightarrow$  **A**), oxidative addition (**A**  $\rightarrow$  **B**), and reductive elimination (**B**  $\rightarrow$  **C**) as shown in Scheme 2. Hard donors ( $\bar{N}$ ,  $\bar{N}$ ) tend to react yielding stable hydrido platinum(IV) complexes **B**,<sup>4</sup> whereas soft donors ( $\bar{P}$ ,  $\bar{P}$ ,  $\bar{S}$ ,  $\bar{S}$ ) tend to react yielding acylplatinum-

Scheme 1



(II) complexes **C**, while the Pt(IV) intermediate **B** may be unseen.<sup>5,6</sup> As for monodentate pyridine and quinoline donors,<sup>6</sup> reaction with 2-(MeOCH<sub>2</sub>)C<sub>5</sub>H<sub>4</sub>N proceeded to give a stable mononuclear platina- $\beta$ -diketone **A**.<sup>7</sup>

Here we report reactions of the platina- $\beta$ -diketone **1** with 2-aminopyridine and 2-(*N*-methylamino)pyridine, which unexpectedly leads to the formation of cyclic aminocarbene complexes of platinum(II). Part of this work has been republished in a Conference Issue.<sup>8</sup>

## 2. Results and Discussion

### 2.1. Synthesis and Spectroscopic Characterization.

The platina- $\beta$ -diketone [Pt<sub>2</sub>{(COMe)<sub>2</sub>H}<sub>2</sub>( $\mu$ -Cl)<sub>2</sub>] (**1**) was found to react with 2 equiv of 2-aminopyridine and 2-(*N*-methylamino)pyridine, respectively, in tetrahydrofuran, yielding aminocarbene complexes of plat-

(1) Steinborn, D.; Gerisch, M.; Merzweiler, K.; Schenzel, K.; Pelz, K.; Bögel, H.; Magull, J. *Organometallics* **1996**, *15*, 2454–2457.

(2) (a) Lukehart, C. M. *Acc. Chem. Res.* **1981**, *14*, 109–116. (b) Lukehart, C. M. *Adv. Organomet. Chem.* **1986**, *25*, 45–71.

(3) (a) Steinborn, D.; Gerisch, M.; Heinemann, F. W.; Bruhn, C. *Chem. Commun.* **1997**, 843–844. (b) Gerisch, M.; Bruhn, C.; Porzel, A.; Steinborn, D. *Eur. J. Inorg. Chem.* **1998**, 1655–1659.

(4) Steinborn, D.; Vyater, A.; Bruhn, C.; Gerisch, M.; Schmidt, H. *J. Organomet. Chem.* **2000**, *597*, 10–16.

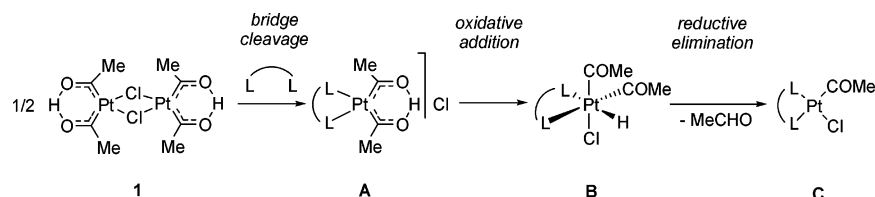
(5) Gosavi, T.; Rusanov, E.; Schmidt, H.; Steinborn, D. *Inorg. Chim. Acta* **2004**, *357*, 1781–1788.

(6) Gerisch, M.; Heinemann, F. W.; Bruhn, C.; Scholz, J.; Steinborn, D. *Organometallics* **1999**, *18*, 564–572.

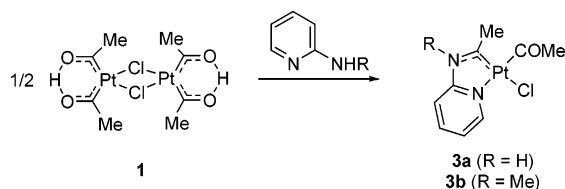
(7) Gosavi, T.; Wagner, C.; Schmidt, H.; Steinborn, D. *J. Organomet. Chem.*, submitted.

(8) Gosavi, T.; Wagner, C.; Rusanov, E.; Schmidt, H.; Steinborn, D. *Monogr. Ser., Int. Conf. Coord. Chem.* **2003**, *6*, 59–64.

## Scheme 2



## Scheme 3



inum(II)  $[\text{Pt}(\text{COMe})\text{Cl}\{2-(\text{CMe}=\text{NR})\text{C}_5\text{H}_4\text{N}-\kappa\text{C},\text{N}\}]$  ( $\text{R} = \text{H}$ , **3a**;  $\text{Me}$ , **3b**) (Scheme 3). The complexes **3** were isolated in moderate yields (45–49%) as slightly air-sensitive pale yellow microcrystalline substances. In the solid state they melt with decomposition at 186–188 °C (**3a**) and 164–166 °C (**3b**). Both complexes are moderately soluble in chloroform, acetone, dichloromethane, and methanol and insoluble in thf, diethyl ether, and pentane.

The identities of complexes **3** were confirmed by microanalysis and by their IR (**3a/3b**:  $\nu(\text{Pt}-\text{Cl})$  304/310  $\text{cm}^{-1}$ ,  $\nu(\text{C}=\text{O})$  1601/1629  $\text{cm}^{-1}$ ),  $^1\text{H}$ , and  $^{13}\text{C}$  NMR spectra. Furthermore, they were also structurally characterized by X-ray diffraction analyses.  $^1\text{H}$  and  $^{13}\text{C}$  NMR spectra clearly showed the formation of only one isomer that was unambiguously characterized by X-ray diffraction analysis to have the pyridine and the acetyl ligand in mutual trans position. Assignment of resonances of acetyl carbon and hydrogen atoms is based on comparison with other complexes of the type  $[\text{Pt}(\text{COMe})\text{Cl}(\text{L}'\text{L}')]$  ( $\text{L}'\text{L}' = \text{RSCH}_2\text{CH}_2\text{SR}$ , **4a**;  $2-(\text{RSCH}_2)\text{C}_5\text{H}_4\text{N}$ , **4b**;<sup>5</sup>  $8-(\text{MeS})\text{quin}$ , **4c** (quin = quinoline);  $2-(\text{HOCH}_2)\text{C}_5\text{H}_4\text{N}$ , **4d**;<sup>7</sup>  $4,4'\text{-R}_2\text{-bpy}$ , **4e** (bpy = 2,2'-bipyridine),<sup>9</sup>  $\text{PhN}=\text{CMe}-\text{CMe}=\text{NPh}$ , **4f**;<sup>10</sup>  $\text{Ph}_2\text{P}(\text{CH}_2)_n\text{PPh}_2$ ,  $n = 2, 3$ , **4g**).<sup>6</sup> Although in complexes **4**  $\delta_{\text{C}}(\text{CO})$  was found to be in a wide range between 207 and 244 ppm, the carbonyl carbon atoms were found to resonate at 207–222 ppm when a pyridine-type ligand is trans to the acetyl ligand. Thus, most likely, in complexes **3a** and **3b** the more high-field-shifted resonances (**3a/3b**: 214.7/216.6 ppm) have to be assigned to the acetyl C atoms and the more low-field-shifted resonances (**3a/3b**: 232.0/226.4 ppm) to the carbene C atoms. The resonances  $\delta_{\text{C}}(\text{CH}_3)$  in type **4** complexes showed a smaller dependence on ligand  $\text{L}'\text{L}'$  (40–54 ppm). Thus, the resonances of methyl C atoms at 44.7/44.7 ppm (**3a/3b**) have to be assigned to the acetyl ligands and those at 32.5/31.9 ppm (**3a/3b**) to the carbene ligands.  $\text{C}_\text{H}\text{-COSY}$  measurements of **3a** made clear that the methyl protons of the acetyl ligands are at lower field with lower  $^3J(\text{Pt},\text{H})$  coupling constant (2.44 ppm, 14.26 Hz) than those of the  $\text{Pt}=\text{C}-\text{CH}_3$  group (2.26 ppm, 57.61 Hz). The coupling constants  $^1J(\text{Pt},\text{C})$  to the acetyl carbon atoms

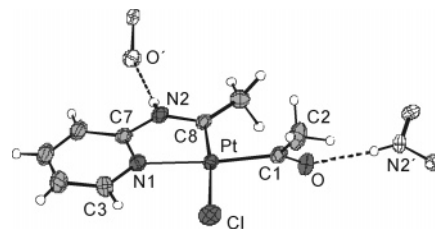


**Figure 1.** Solid state structure of one of the two symmetry-independent molecules of  $[\text{Pt}(\text{COMe})\text{Cl}\{2-(\text{CMe}=\text{NH})\text{C}_5\text{H}_4\text{N}\}]\cdot\text{CD}_3\text{OD}$  (**3a**· $\text{CD}_3\text{OD}$ ) along with the numbering scheme (displacement ellipsoids at 30% probability). Hydrogen bonds to the other symmetry-independent molecule are shown (see text). The solvate molecule is not shown for clarity.

**Table 1.** Selected Bond Lengths (in Å) and Angles (in deg) for **3a**· $\text{CD}_3\text{OD}$ <sup>a</sup>

Pt–C1	1.982(6)/1.981(6)	Pt–N1	2.138(5)/2.132(5)
Pt–Cl	2.364(2)/2.369(2)	Pt–C8	1.944(6)/1.943(6)
N2–C8	1.331(7)/1.340(7)	C1–O	1.227(7)/1.219(7)
N1–Pt–Cl	94.2(2)/93.8(1)	N1–Pt–C8	79.1(2)/80.0(2)
C8–Pt–C1	95.0(2)/94.8(2)	C1–Pt–Cl	91.8(2)/91.4(2)
C8–Pt–Cl	172.8(2)/173.6(2)	N1–Pt–C1	173.7(2)/174.7(2)

<sup>a</sup> Values for the two symmetry-independent molecules are given separated by a slash.

(**3a/3b**: 1494.2/1534.4 Hz) are much higher than those in complexes **4** with the pyridine-type donor in trans position (867–989 ppm). This indicates a low trans influence of the pyridine moiety in **3a/3b**, possibly due to the electronic withdrawing effect of the carbene substituent.

**2.2. Molecular Structures.** Single crystals suitable for X-ray structure diffraction analyses were obtained from  $\text{CD}_3\text{OD}$  (**3a**) and  $\text{CD}_2\text{Cl}_2$  (**3b**) solutions. Complex **3a** crystallizes with one molecule of  $\text{CD}_3\text{OD}$ . The asymmetric unit contains two symmetry-independent molecules. They are very similar in molecular structure. One of them is shown in Figure 1; selected bond lengths and angles are listed in Table 1. In the crystal molecules are connected through hydrogen bonds where the N–H groups act as hydrogen donors and the acetyl ligands as hydrogen acceptors (see Figure 1):  $\text{N}2\cdots\text{O}'$ :  $\text{N}2\cdots\text{O}'$  2.828(7) Å,  $\text{N}2\text{--H}$  0.76 Å,  $\text{H}\cdots\text{O}'$  2.08 Å,  $\text{N}2\text{--H}\cdots\text{O}'$  169°;  $\text{N}2'\text{--H}'\cdots\text{O}$ :  $\text{N}2'\cdots\text{O}$  2.793(7) Å,  $\text{N}2'\text{--H}'$  0.77 Å,  $\text{H}'\cdots\text{O}$  2.02 Å,  $\text{N}2'\text{--H}'\cdots\text{O}$  174°. Complex **3b** crystallizes as discrete molecules without unusual intermolecular interactions (shortest intermolecular contact between non-hydrogen atoms:  $\text{O}\cdots\text{C}7'$  3.03(1) Å). The molecular structure is shown in Figure 2; selected structural parameters are given in Table 2.

In both complexes the platinum atom has a square-planar coordination (configuration index  $SP\text{-}4\text{-}4$ ). The acetyl ligands include angles with complex planes of 60.8(7)/62.5(8)° (**3a**) and 71(1)° (**3b**). The five-membered  $\text{Pt}-\text{C}-\text{N}-\text{C}-\text{N}$  rings are planar in good approximation;

(9) Gerisch, M.; Bruhn, C.; Vyater, A.; Davies, J. A.; Steinborn, D. *Organometallics* **1998**, *17*, 3101–3104.

(10) Vyater, A.; Wagner, C.; Merzweiler, K.; Steinborn, D. *Organometallics* **2002**, *21*, 4369–4376.

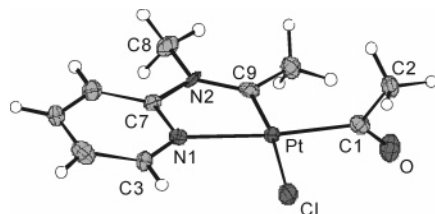


**Figure 2.** Molecular structure of  $[\text{Pt}(\text{COMe})\text{Cl}\{2-(\text{CMe}=\text{NR})\text{C}_5\text{H}_4\text{N}\}]$  in crystals of **3b** along with the numbering scheme (displacement ellipsoids at 30% probability).

**Table 2. Selected Bond Lengths (in Å) and Angles (in deg) for **3b****

Pt–C1	2.00(1)	Pt–N1	2.120(8)
Pt–Cl	2.369(2)	Pt–C9	1.950(9)
N2–C9	1.31(1)	C1–O	1.21(1)
N1–Pt–Cl	94.6(2)	N1–Pt–C9	79.0(3)
C9–Pt–C1	96.9(4)	C1–Pt–Cl	89.6(3)
N1–Pt–C1	174.5(3)	C9–Pt–Cl	173.2(3)

greatest deviations from the mean planes are  $<0.05$  Å. The Pt–C<sub>carbene</sub> bond lengths (1.944(6)/1.943(6) Å, **3a**; 1.950(9) Å, **3b**) are in the range that was reported for other aminocarbene complexes of Pt(II) (median 2.021 Å, lower/upper quartile 1.938/2.059 Å,  $n = 11$ ;  $n =$  number of observations).<sup>11</sup> Furthermore, comparison with bond lengths Pt(II)–C<sub>sp<sup>2</sup></sub> in aryl and vinyl complexes of platinum(II) (median 2.044, lower/upper quartile 2.006/2.070 Å,  $n = 998$ )<sup>11</sup> indicates that Pt–C bonds in **3a** and **3b** are shortened due to partial  $d_{\pi}$ – $p_{\pi}$  bonding. The N–C<sub>carbene</sub> bonds (1.331(7)/1.340(7) Å, **3a**; 1.31(1) Å, **3b**) are as long as the C–N bonds in pyridine (1.331–1.338 Å).<sup>12</sup> This is clear evidence for a substantial  $p_{\pi}$ – $p_{\pi}$  double bonding in the N–C<sub>carbene</sub> bonds.

**2.3. Computational Results.** To get insight into the gas phase structures of aminocarbene complexes **3**, quantum chemical calculations on the DFT level of theory were performed. Geometry optimization without any symmetry restriction led to the calculated equilibrium structures **3a<sub>calc</sub>** and **3b<sub>calc</sub>**, which are shown in Figure 3; selected structural parameters are given in Table 3.

Calculations reproduce experimentally found structures quite well, except for the Pt–N bonds (**3a**: calc 2.256 Å, expt 2.138(5)/2.132(5) Å; **3b**: calc 2.211 Å, expt 2.120(8) Å) and the angles between the acetyl ligands and complex planes (**3a**: calc 49.0°, expt 60.8(7)/62.5(8)°; **3b**: calc 50.1°, expt 71(1)°). As an example, for **3a<sub>calc</sub>** scans of the potential energy surface for the Pt–N1 coordinate as well as for the C2–C1–Pt–C8 coordinate (being a measure of the interplanar angle between the acetyl ligand and the complex plane) were performed. Figure 4 exhibits that the energy demand to bring the Pt–N1 bond length and the dihedral angle C2–C1–Pt–C8 from the calculated up to the experimentally found values is only about 1.5 and 0.5 kcal/mol, respectively. Thus, structural differences between calculated and experimental structures may be caused, at least in part, by packing effects in the crystal.

The five-membered platinacycles having incorporated the aminocarbene units are planar in very good ap-

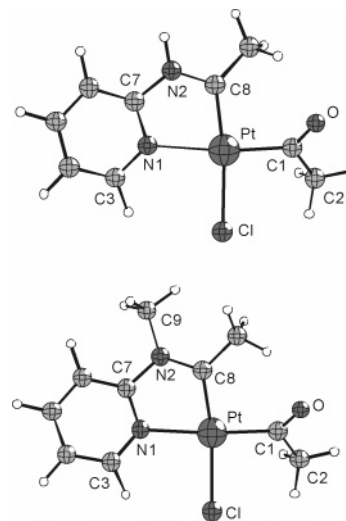


**Figure 3.** Calculated structures of  $[\text{Pt}(\text{COMe})\text{Cl}\{2-(\text{CMe}=\text{NR})\text{C}_5\text{H}_4\text{N}\}]$  (top: R = H, **3a<sub>calc</sub>**; bottom: R = Me, **3b<sub>calc</sub>**) along with the numbering schemes.

**Table 3. Calculated Bond Lengths (in Å) and Angles (in deg) for Aminocarbene Complexes **3a<sub>calc</sub>** and **3b<sub>calc</sub>****

	<b>3a<sub>calc</sub></b>	<b>3b<sub>calc</sub></b>
Pt–C1/BO <sup>a</sup>	2.015/0.740	2.019/0.732
Pt–C8/BO	1.946/0.871	1.953/0.870
Pt–Cl/BO	2.389/0.381	2.397/0.374
Pt–N1/BO	2.256/0.176	2.211/0.191
N2–C8/BO	1.353/1.296	1.365/1.278
N2–C7/BO	1.404/1.044	1.419/1.028
C1–O/BO	1.218/1.787	1.219/1.771
N1–Pt–C1	173.6	175.0
Cl–Pt–C8	170.5	170.2
N1–Pt–C8	78.4	78.3

<sup>a</sup> BO = bond order, Wiberg bond index (given in electron pairs).

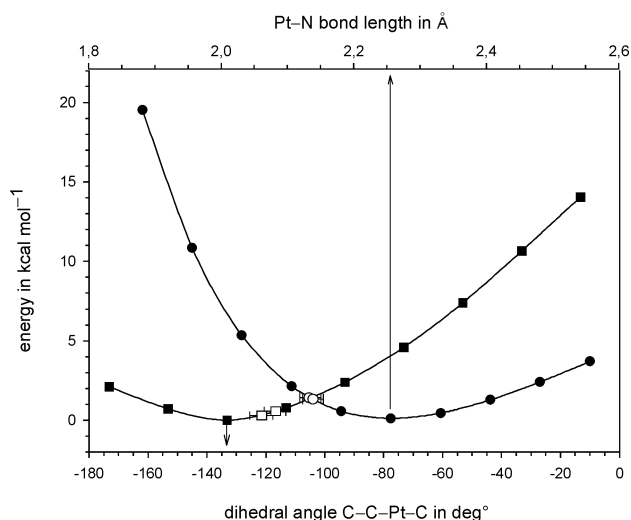


**Figure 4.** Scans of the potential energy surface for the Pt–N1 (●) and C2–C1–Pt–C8 (■) coordinates for the molecule **3a<sub>calc</sub>**. Values of the equilibrium structure **3a<sub>calc</sub>** are marked by arrows. Experimentally found values along with their error bars ( $\pm 3\sigma$ ) for the two symmetry-independent molecules in crystals of **3a**·CD<sub>3</sub>OD are given by open circles (○) and squares (□), respectively.

(11) Cambridge Structural Database (CSD); Cambridge Crystallographic Data Centre, University Chemical Laboratory: Cambridge, U.K.

(12) Mootz, D.; Wussow, H.-G. *J. Chem. Phys.* **1981**, *75*, 1517–1522.

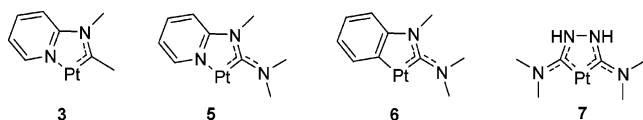
proximation (greatest deviation from the mean plane:  $<0.003$  Å for **3a<sub>calc</sub>** and  $<0.03$  Å for **3b<sub>calc</sub>**). Besides the shortening of the Pt–C<sub>carbene</sub> (Pt–C8) and N–C<sub>carbene</sub>

**Table 4. Charge Decomposition Analysis of the Pt–C<sub>carbene</sub> and Pt–N Bonds in Cyclic Aminocarbene Complexes [Pt(COMe)Cl{2-(CMe==NR)C<sub>5</sub>H<sub>4</sub>N}] (**3a/b**<sub>calc</sub>) and in [Pt(COMe)Cl(CMe==NMeH)py] (**3c**<sub>calc</sub>) for Comparison (values in electrons)**

complex	donation	back-donation	repulsive polarization	residual term
[Pt(COMe)Cl{2-(CMe==NH)C <sub>5</sub> H <sub>4</sub> N}] ( <b>3a</b> <sub>calc</sub> )	0.459	0.241	−0.695	−0.110
[Pt(COMe)Cl{2-(CMe==NMe)C <sub>5</sub> H <sub>4</sub> N}] ( <b>3b</b> <sub>calc</sub> )	0.434	0.255	−0.751	−0.104
[Pt(COMe)Cl(CMe==NMeH)py] ( <b>3c</b> <sub>calc</sub> ) <sup>a</sup>	0.405	0.236	−0.477	−0.096
[Pt(COMe)Cl(CMe==NMeH)py] ( <b>3c</b> <sub>calc</sub> ) <sup>b</sup>	0.236	0.001	−0.319	−0.011

<sup>a</sup> CDA of the carbene ligand onto the Pt(COMe)(Cl)py fragment. <sup>b</sup> CDA of the pyridine ligand onto the Pt(COMe)Cl(CMe==NMeH) fragment.

#### Scheme 4



(N2–C8) bonds (see discussion in section 2.2), the bond orders of these two bonds (Table 3) also reflect their partial  $d_{\pi}-p_{\pi}$  (Pt–C) and  $p_{\pi}-p_{\pi}$  (N–C) double-bond character. As expected for Fischer-type carbene complexes, the carbene carbon atoms (C8) bear a positive charge (+0.170, **3a**<sub>calc</sub>; +0.184, **3b**<sub>calc</sub>; charges given in electrons). This bonding model is further supported by the charge decomposition analysis (CDA) of Frenking (Table 4).<sup>13</sup>

The CDA in the complexes **3a**<sub>calc</sub> and **3b**<sub>calc</sub> between the 2-(CMe==NR)C<sub>5</sub>H<sub>4</sub>N ligands (R = Me, H) and the platinum fragment Pt(COMe)Cl describes the electronic changes associated with the formation both the Pt–C<sub>carbene</sub> and the Pt–N<sub>py</sub> bonds. There was found a substantial  $\pi$  back-donation that has to be ascribed solely to the platinum–carbene bonds. The proof that the pyridine N-donor site is purely  $\sigma$  bonded came from calculations on the same level of theory of the hypothetical complex [Pt(COMe)Cl(CMe==NMeH)py] (**3c**<sub>calc</sub>) having two monodentate ligands, namely, the carbene ligand CMe==NMeH and the pyridine ligand (Table 4). The magnitude of the  $\pi$  back-donation (Pt→C<sub>carbene</sub>, **3a/b**<sub>calc</sub>: 0.241/0.255 electrons) is in the range found in other Fischer-type carbene complexes.<sup>14</sup> Furthermore, the nonvanishing residual terms indicate that for a full understanding of the Pt–C<sub>carbene</sub> bonds besides the donor–acceptor interactions (just discussed) covalent interactions between open-shell fragments should also be considered.

**2.4. Discussion.** Characteristic features of aminocarbeneplatinum(II) complexes **3** formed in the reactions of platina- $\beta$ -diketone **1** with 2-aminopyridines (Scheme 3) are chelate ligands with a pyridine and a carbene donor site. Comparison of complexes **3** with other five-membered platinacycles having incorporated aminocarbene donor sites (Scheme 4) exhibits that complexes **3** contain mono-N-functionalized carbene ligands, whereas complexes described in the literature, such as type **5**,<sup>15</sup> **6**,<sup>16,17</sup> and **7**<sup>15a,18</sup> complexes, contain di-N-functionalized carbene ligands.

A tentative mechanism for the unexpected formation of aminocarbene complexes **3** in reactions of platina- $\beta$ -

diketone **1** with 2-(RHN)C<sub>5</sub>H<sub>4</sub>N (R = H, Me) is shown in Scheme 5. Most likely, the first step is the cleavage of the Pt–Cl–Pt bridges resulting in the formation of mononuclear platina- $\beta$ -diketone complexes **8**. Analogously, complex **1** was found to react with pyridine and quinoline, yielding complexes of that type, [Pt{(COMe)<sub>2</sub>H}Cl(L)] (L = pyridine, quinoline), as the principal products.<sup>6</sup>

Then, aminocarbene complexes **3** should be formed by intramolecular attack of the amino group to the hydroxycarbene carbon atom (**8** → **3**). An analogous intermolecular transformation, namely, the conversion of oxycarbene into aminocarbene complexes, is one of the “classics” for Fischer-type carbene complexes.<sup>19</sup> They are also typical for Lukehart’s metalla- $\beta$ -diketones<sup>2</sup> but were never observed before for the platina- $\beta$ -diketone **1**. These new reactions for type **1** complexes seem to proceed because the usual reaction pathway (see Scheme 2: **1** → **A** → **B**) may be hampered due to the formation of an energetically unfavorable four-mem-

bered Pt–N–C–N cycle in type **9** complexes (Scheme 5). We failed to get in the same way as complexes **3** oxycarbene and thiocarbene complexes in reactions of **1** with 2-hydroxypyridine and 2-mercaptopyridine. Most likely, this is due to predominance of the keto (thio keto) form (**D**, Y = O, S) in the tautomerism, whereas in 2-aminopyridines the amino form (**E**, YH = NHR, R = H, Me) is predominant (Scheme 6).<sup>20,21</sup>

Summarizing, the formation of the aminocarbene-platinum(II) complexes **3a/b** described herein is the first example where the electronically unsaturated and kinetically labile platina- $\beta$ -diketone **1** exhibits a reactivity that is closely analogous to that of the electronically saturated and kinetically inert Lukehart’s metalla- $\beta$ -diketones **2**.

### 3. Experimental Section

**3.1. General Comments.** All reactions were performed under an Ar atmosphere using standard Schlenk techniques. Solvents were dried (Et<sub>2</sub>O and thf over Na-benzophenone) and distilled prior to use. <sup>1</sup>H and <sup>13</sup>C NMR spectra were recorded on Varian VXR 400 and Unity 500 NMR spectrometers.

(16) (a) Zhang, S.-W.; Ishii, R.; Motoori, F.; Tanaka, T.; Takai, Y.; Sawada, M.; Takahashi, S. *Inorg. Chim. Acta* **1997**, *265*, 75–82. (b) Zhang, S.-W.; Kaharu, T.; Pirio, N.; Ishii, R.; Uno, M.; Takahashi, S. *J. Organomet. Chem.* **1995**, *489*, C62–C64.

(17) Hiraki, K.; Onishi, M.; Ohnuma, K.; Sugino, K. *J. Organomet. Chem.* **1981**, *416*, 413–419.

(18) Lai, S.-W.; Chan, M. C. W.; Wang, Y.; Lam, H.-W.; Peng, S.-M.; Che, C.-M. *J. Organomet. Chem.* **2001**, *617–618*, 133–140, and references therein.

(19) (a) Fischer, E. O. *Pure Appl. Chem.* **1970**, *24*, 407–423. (b) Fischer, E. O. *Angew. Chem.* **1974**, *86*, 651–663.

(20) Stefaniak, L. *Tetrahedron* **1976**, *32*, 1065–1067.

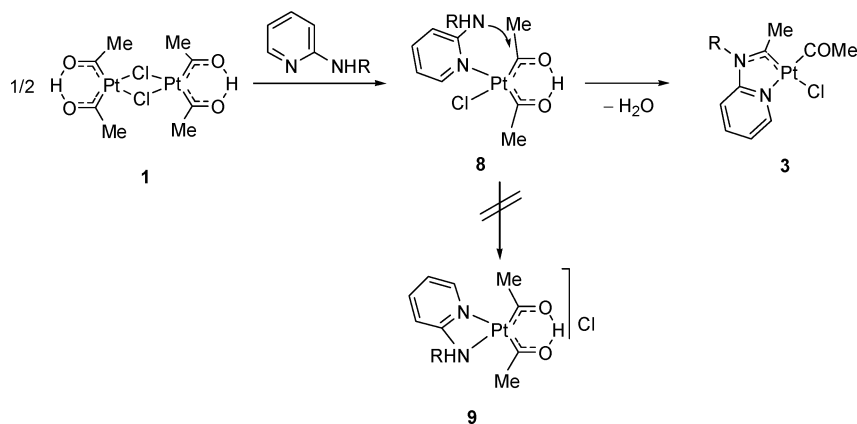
(21) Stefaniak, L. *Org. Magn. Reson.* **1979**, *12*, 379–382.

(13) Dapprich, S.; Frenking, G. *J. Phys. Chem.* **1995**, *99*, 9352–9362.

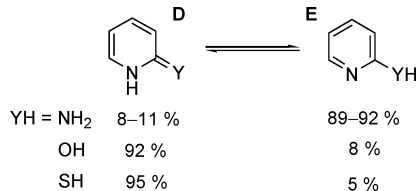
(14) (a) Vyboishchikov, S. F.; Frenking, G. *Chem. Eur. J.* **1998**, *4*, 1428–1438. (b) Frenking, G.; Fröhlich, N. *Chem. Rev.* **2000**, *100*, 717–774.

(15) (a) Balch, A. L.; Parks, J. E. *J. Am. Chem. Soc.* **1974**, *96*, 4114–4121. (b) Crociani, B.; Richards, R. L. *J. Chem. Soc., Dalton Trans.* **1974**, 693–697.

Scheme 5



Scheme 6



Chemical shifts are relative to  $\text{CHCl}_3$  ( $\delta$  7.24) and  $\text{CDCl}_3$  ( $\delta$  77.0) as internal references. Assignments of NMR signals were partly revealed by COSY experiments ( $^1\text{H}, ^1\text{H}$ ;  $^1\text{H}, ^{13}\text{C}$ ) and by running spectra in APT mode. IR spectra were recorded on a Galaxy Mattson 5000 FT-IR spectrometer using CsBr pellets. Microanalyses were performed by the University of Halle microanalysis laboratory using CHNS-932 (LECO) and Vario EL (Elementar Analysensysteme) elemental analyzers. The complex  $[\text{Pt}_2\{(\text{COMe})_2\text{H}\}_2(\mu\text{-Cl})_2]$  (**1**) was synthesized according to a published method.<sup>1</sup>

**3.2. Syntheses of  $[\text{Pt}(\text{COMe})\text{Cl}\{2\text{-}(\text{CMe}=\text{NR})\text{C}_5\text{H}_4\text{N}\}]$  (**3**).** To a suspension of  $[\text{Pt}_2\{(\text{COMe})_2\text{H}\}_2(\mu\text{-Cl})_2]$  (**1**) (50 mg, 0.08 mmol) in thf (4 mL), cooled to  $-40$  °C, was added 2-(NHR)- $\text{C}_5\text{H}_4\text{N}$  (R = H, Me) (0.16 mmol). The pale yellow suspension immediately changed color to an intense yellow solution. The reaction mixture was warmed to room temperature within 10–20 min, resulting in the formation of a yellow precipitate. Then diethyl ether (10–15 mL) was added to complete the product precipitation. Finally the precipitate was filtered off, washed with diethyl ether (5 mL), and dried briefly in vacuo.

**Complex 3a** (R = H). Yield: 31 mg (49%). Mp: 186–188 °C (dec). Anal. Calc for  $\text{C}_9\text{H}_{11}\text{ClN}_2\text{OPt}$  (393.75): C, 27.45; H, 2.82; N, 7.11; Cl, 9.00. Found: C, 27.18; H, 2.82; N, 7.06; Cl, 8.84. IR (CsBr):  $\nu(\text{C}=\text{O})$  1601,  $\nu(\text{Pt}-\text{Cl})$  304  $\text{cm}^{-1}$ .  $^1\text{H}$  NMR (400 MHz,  $\text{CD}_3\text{OD}$ ):  $\delta$  2.26 (s + d,  $^3J(\text{Pt},\text{H}) = 57.61$  Hz, 3H,  $\text{CCH}_3$ ), 2.44 (s + d,  $^3J(\text{Pt},\text{H}) = 14.26$  Hz, 3H,  $\text{COCH}_3$ ), 7.47 (d,  $^3J(\text{H}_3,\text{H}_4) = 8.20$  Hz, 1H, 3- $\text{CH}_{\text{py}}$ ), 7.65 (ddd,  $^3J(\text{H}_5,\text{H}_4) = 7.62$  Hz,  $^3J(\text{H}_5,\text{H}_6) = 5.47$  Hz,  $^4J(\text{H}_5,\text{H}_3) = 0.98$  Hz, 1H, 5- $\text{CH}_{\text{py}}$ ), 8.16 (ddd,  $^3J(\text{H}_4,\text{H}_3) = ^3J(\text{H}_4,\text{H}_5) = 7.86$  Hz,  $^4J(\text{H}_4,\text{H}_6) = 1.57$  Hz, 1H, 4- $\text{CH}_{\text{py}}$ ), 8.93 (ddd,  $^3J(\text{H}_6,\text{H}_5) = 5.47$  Hz,  $^4J(\text{H}_6,\text{H}_4) = 1.57$  Hz,  $^5J(\text{H}_6,\text{H}_3) = 0.78$  Hz, 1H, 6- $\text{CH}_{\text{py}}$ ), resonance for N–H not observed.  $^{13}\text{C}$  NMR (100 MHz,  $\text{CD}_3\text{OD}$ ):  $\delta$  32.5 (s,  $\text{CCH}_3$ ), 44.7 (s + d,  $^2J(\text{Pt},\text{C}) = 232.1$  Hz,  $\text{COCH}_3$ ), 113.7 (s, 3- $\text{C}_{\text{py}}$ ), 124.0 (s, 5- $\text{C}_{\text{py}}$ ), 143.4 (s, 4- $\text{C}_{\text{py}}$ ), 148.2 (s + d,  $^2J(\text{Pt},\text{C}) = 17.6$  Hz, 6- $\text{C}_{\text{py}}$ ), 156.6 (s, 2- $\text{C}_{\text{py}}$ ), 214.7 (s + d,  $^1J(\text{Pt},\text{C}) = 1494.2$  Hz,  $\text{COCH}_3$ ), 232.0 (s,  $\text{CCH}_3$ ).

**Complex 3b** (R = Me). Yield: 29 mg (45%). Mp: 164–166 °C (dec). Anal. Calc for  $\text{C}_{10}\text{H}_{13}\text{ClN}_2\text{OPt}$  (407.75): C, 29.46; H, 3.21; N, 6.87; Cl, 8.69. Found: C, 29.32; H, 3.17; N, 6.80; Cl, 8.57. IR (CsBr):  $\nu(\text{C}=\text{O})$  1629,  $\nu(\text{Pt}-\text{Cl})$  310  $\text{cm}^{-1}$ .  $^1\text{H}$  NMR (400 MHz,  $\text{CD}_2\text{Cl}_2$ ):  $\delta$  2.32 (s + d, partially overlapped,  $^3J(\text{Pt},\text{H}) = 60.40$  Hz, 3H,  $\text{CCH}_3$ ), 2.37 (s + d,  $^3J(\text{Pt},\text{H}) = 12.82$  Hz, 3H,  $\text{COCH}_3$ ), 3.47 (s, 3H, N- $\text{CH}_3$ ), 7.41 (d,  $^3J(\text{H}_3,\text{H}_4) =$

Table 5. Crystallographic and Data Collection Parameters for Compounds **3a**· $\text{CD}_3\text{OD}$  and **3b**

	<b>3a</b> · $\text{CD}_3\text{OD}$	<b>3b</b>
empirical formula	$\text{C}_{19}\text{H}_{22}\text{Cl}_2\text{N}_4\text{O}_3\text{Pt}_2$	$\text{C}_{10}\text{H}_{13}\text{ClN}_2\text{OPt}$
$M_r$	815.49	407.76
cryst size (mm)	$0.21 \times 0.19 \times 0.18$	$0.09 \times 0.09 \times 0.07$
cryst syst	monoclinic	monoclinic
space group	$P2_1/c$	$P2_1/n$
$a/\text{Å}$	13.193(3)	9.487(2)
$b/\text{Å}$	12.847(2)	9.200(2)
$c/\text{Å}$	14.335(3)	13.979(3)
$\beta/\text{deg}$	98.36(3)	105.92(2)
$V/\text{Å}^3$	2403.8(9)	1173.3(4)
$Z$	4	4
$D_{\text{calc}}/\text{g cm}^{-3}$	2.253	2.308
$\mu(\text{Mo K}\alpha)/\text{mm}^{-1}$	11.875	12.162
$F(000)$	1512	760
$\theta$ range/deg	2.14–25.93	2.68–25.00
no. of refls collected	18 287	6028
no. of refls obsd	3429	1526
$[I > 2\sigma(I)]$		
no. of indep refls	4638 ( $R_{\text{int}} = 0.0480$ )	2058 ( $R_{\text{int}} = 0.0697$ )
no. of data/restraints/params	4638/0/369	2058/0/140
goodness-of-fit on $F^2$	0.974	1.033
$R_1, wR_2 [I > 2\sigma(I)]$	0.0250, 0.0520	0.0304, 0.0726
$R_1, wR_2$ (all data)	0.0420, 0.0562	0.0460, 0.0765
largest diff peak and hole/ $e \text{ Å}^{-3}$	0.780 and $-0.883$	1.129 and $-1.968$

8.46 Hz, 1H, 3- $\text{CH}_{\text{py}}$ ), 7.44 (ddd,  $^3J(\text{H}_5,\text{H}_4) = 7.57$  Hz,  $^3J(\text{H}_5,\text{H}_6) = 5.29$  Hz,  $^4J(\text{H}_5,\text{H}_3) = 0.93$  Hz, 1H, 5- $\text{CH}_{\text{py}}$ ), 8.06 (ddd,  $^3J(\text{H}_4,\text{H}_3) = 8.46$  Hz,  $^3J(\text{H}_4,\text{H}_5) = 7.57$  Hz,  $^4J(\text{H}_4,\text{H}_6) = 1.82$  Hz, 1H, 4- $\text{CH}_{\text{py}}$ ), 8.77 (ddd,  $^3J(\text{H}_6,\text{H}_5) = 5.30$  Hz,  $^4J(\text{H}_6,\text{H}_4) = 1.77$  Hz,  $^5J(\text{H}_6,\text{H}_3) = 0.73$  Hz, 1H, 6- $\text{CH}_{\text{py}}$ ).  $^{13}\text{C}$  NMR (126 MHz,  $\text{CD}_3\text{NO}_2$ ):  $\delta$  31.9 (s + d,  $^2J(\text{Pt},\text{C}) = 184.5$  Hz,  $\text{CCH}_3$ ), 36.9 (s + d,  $^3J(\text{Pt},\text{C}) = 46.9$  Hz, N- $\text{CH}_3$ ), 44.7 (s + d,  $^2J(\text{Pt},\text{C}) = 234.4$  Hz,  $\text{COCH}_3$ ), 114.4 (s, 3- $\text{C}_{\text{py}}$ ), 124.8 (s, 5- $\text{C}_{\text{py}}$ ), 143.3 (s, 4- $\text{C}_{\text{py}}$ ), 148.0 (s, 6- $\text{C}_{\text{py}}$ ), 158.6 (s + d,  $^{2+3}J(\text{Pt},\text{C}) = 74.8$  Hz, 2- $\text{C}_{\text{py}}$ ), 216.6 (s + d,  $^1J(\text{Pt},\text{C}) = 1534.4$  Hz,  $\text{COCH}_3$ ), 226.4 (s + d,  $^1J(\text{Pt},\text{C}) = 1139.9$  Hz,  $\text{CCH}_3$ ).

**3.3. X-ray Structure Determinations.** Intensity data were collected on a STOE IPDS diffractometer at 220(2) K using graphite-monochromatized Mo K $\alpha$  radiation ( $\lambda = 0.71073$  Å). A summary of the crystallographic data, the data collection parameters, and the refinement parameters is given in Table 5. Absorption correction was applied numerically ( $T_{\text{min}}/T_{\text{max}}$  0.1118/0.2157, **3a**; 0.3532/0.4744, **3b**). The structures were solved by direct methods with SHELXS-97<sup>22</sup> and refined using full-matrix least-squares routines against  $F^2$  with SHELXL-97.<sup>22</sup> Non-hydrogen atoms were refined with aniso-

(22) Sheldrick, G. M. SHELXS-97, SHELXL-97, Programs for Structure Determination; University of Göttingen: Göttingen, Germany, 1990, 1997.

tropic and hydrogen atoms with isotropic displacement parameters. The H atoms were added to the model in calculated positions according to the riding model (**3a**) and were found in the difference Fourier map (**3b**), respectively. In the case of **3a**-CD<sub>3</sub>OD, the oxygen atom of CD<sub>3</sub>OD is disordered over two positions (occupancies: 65/35%); the D atoms of CD<sub>3</sub>OD were not found and not included in the model.

**3.4. Computational Details.** All DFT calculations were carried out using the Gaussian98 program package<sup>23</sup> with the hybrid functional B3LYP.<sup>24</sup> For the main group atoms the basis 6-31G(d,p) was employed. The valence shell of platinum has been approximated by a split valence basis set too; for its core orbitals an effective core potential in combination with consideration of relativistic effects has been used.<sup>25</sup> All systems have been fully optimized without any symmetry restrictions.

(23) Frisch, M. J.; Trucks, G. W.; Schlegel, H. B.; Scuseria, G. E.; Robb, M. A.; Cheeseman, J. R.; Zakrzewski, V. G.; Montgomery, Jr., J. A.; Stratmann, R. E.; Burant, J. C.; Dapprich, S.; Millam, J. M.; Daniels, A. D.; Kudin, K. N.; Strain, M. C.; Farkas, O.; Tomasi, J.; Barone, V.; Cossi, M.; Cammi, R.; Mennucci, B.; Pomelli, C.; Adamo, C.; Clifford, S.; Ochterski, J.; Petersson, G. A.; Ayala, P. Y.; Cui, Q.; Morokuma, K.; Malick, D. K.; Rabuck, A. D.; Raghavachari, K.; Foresman, J. B.; Cioslowski, J.; Ortiz, J. V.; Stefanov, B. B.; Liu, G.; Liashenko, A.; Piskorz, P.; Komaromi, I.; Gomperts, R.; Martin, R. L.; Fox, D. J.; Keith, T.; Al-Laham, M. A.; Peng, C. Y.; Nanayakkara, A.; Gonzalez, C.; Challacombe, M.; Gill, P. M. W.; Johnson, B.; Chen, W.; Wong, M. W.; Andres, J. L.; Gonzalez, C.; Head-Gordon, M.; Replogle, E. S.; Pople, J. A. *Gaussian 98, Revision A.3*; Gaussian Inc.: Pittsburgh, PA, 1998.

(24) (a) Becke, A. D. *Phys. Rev. A* **1988**, *38*, 3098–3100. (b) Becke, A. D. *J. Chem. Phys.* **1993**, *98*, 5648–5652. (c) Lee, C.; Yang, W.; Parr, R. G. *Phys. Rev. B* **1988**, *37*, 785–789. (d) Stephens, P. J.; Devlin, F. J.; Chabalowski, C. F.; Frisch, M. J. *J. Phys. Chem.* **1994**, *98*, 11623–11627.

(25) Andrae, D.; Häussermann, U.; Dolg, M.; Stoll, H.; Preuss, H. *Theor. Chim. Acta* **1990**, *77*, 123–141.

The resulting geometries were characterized as equilibrium structures by the analysis of the force constants of normal vibrations. Atomic charges and bond orders were obtained by the natural bond orbital (NBO) analysis of Reed et al.<sup>26</sup> as implemented in Gaussian98. The charge decomposition analyses (CDA) were performed with the program CDA2.1 by Dapprich and Frenking.<sup>27</sup>

Crystallographic data (excluding structure factors) have been deposited at the Cambridge Crystallographic Data Center as supplementary publication nos. CCDC-260201 (**3a**) and CCDC-360202 (**3b**). Copies of the data can be obtained free of charge on application to CCDC, 12 Union Road, Cambridge, CB2, 1EZ, UK [fax: (internat.) +44(0)1223/336–033; e-mail: deposit@ccdc.cam.ac.uk].

**Acknowledgment.** We gratefully acknowledge support by the Deutsche Forschungsgemeinschaft. We also thank the Merck (Darmstadt) for gifts of chemicals.

**Supporting Information Available:** X-ray crystallographic data are available as CIF files. Tables of Cartesian coordinates of atom positions calculated for equilibrium structures **3a**<sub>calc</sub>, **3b**<sub>calc</sub>, and **3c**<sub>calc</sub> as well as a scan of the potential energy surface for the Pt–N1 and C2–C1–Pt–C8 coordinates for **3a**<sub>calc</sub>. This material is available free of charge via the Internet at <http://pubs.acs.org>.

OM049191V

(26) Reed, A. E.; Weinstock, R. B.; Weinhold, F. *J. Chem. Phys.* **1985**, *83*, 735–746.

(27) Dapprich, S.; Frenking, G. *CDA2.1*, version 2.1.2; University of Marburg: Marburg, Germany, 2003.